Journal of Nuclear Materials 385 (2009) 623–628

Contents lists available at ScienceDirect

Journal of Nuclear Materials

journal homepage: www.elsevier.com/locate/jnucmat

Amorphization of the interaction products in U–Mo/Al dispersion fuel during irradiation

Ho Jin Ryu [a,*], Yeon Soo Kim [b], G.L. Hofman [b]

[a] Korea Atomic Energy Research Institute, Recycled Fuel Development Division, 150 Deokjin-Dong, Yuseong, Daejeon 305-353, Republic of Korea
[b] Argonne National Laboratory, 9700 S. Cass Ave, Argonne, IL 60439, USA

ARTICLE INFO

Article history:
Received 16 September 2008
Accepted 20 January 2009

ABSTRACT

The microstructures of the product resulting from interaction between U–Mo fuel particles and the Al matrix in U–Mo/Al dispersion fuel are discussed. We analyzed the available characterization results for the Al matrix dispersion fuels from both the out-of-pile and in-pile tests and examined the difference between these results. The morphology of pores that form in the interaction products during irradiation is similar to the porosity previously observed in irradiation-induced amorphized uranium compounds. The available diffraction studies for the interaction products formed in both the out-of-pile and in-pile tests are analyzed. We have concluded that the interaction products in the U–Mo/Al dispersion fuel are formed as an amorphous state or become amorphous during irradiation, depending on the irradiation conditions.

1. Introduction

Because of the high uranium density and good irradiation stability of U–Mo alloys, this fuel in the form of a dispersion in an Al matrix is the choice for the conversion of research reactors and test reactors, currently using highly-enriched uranium (HEU), to low-enriched uranium (LEU) [1,2]. The formation of an interaction layer between U–Mo particles and the Al matrix as a result of interdiffusion has become a major issue for the performance of this fuel. The formation of an interaction product in this dispersion fuel is unfavorable because of its low thermal conductivity and volume expansion as it consumes the Al matrix. Depended on the irradiation conditions (e.g. high burnup or high heat flux), large pores are formed at the interface of the interaction products and the Al matrix (Fig. 1) [3,4], which could eventually lead to a fuel plate failure. The evolution of the pore formation, although the location in the meat is different, closely resembles the fission gas-related pore formation previously observed in amorphized irradiated fuel material such as U_6Fe and U_3Si during irradiation [5]. By analogy, the excessive pore growth that leads to a fuel plate failure is considered the result of irradiation-induced low viscosity of the amorphized irradiated interaction products. No direct characterization of the interaction products of U–Mo/Al dispersion fuel after irradiation has been available until recently.

In this paper, we have analyzed the available results from out-of-pile and in-pile tests of U–Mo, UAl_x, and U_3Si_2 dispersion fuel, and compared the findings from in-pile and out-of-pile tests. We found that the interaction products from the in-pile tests are very different from those formed in the out-of-pile diffusion experiments. This can be explained if the interaction products formed in-pile are amorphous under a certain irradiation condition. Recent papers [6–8] providing neutron and electron diffraction data on irradiated U–Mo dispersion fuel are consistent with our view that the interaction products are amorphous under typical irradiation conditions for a plate-type fuel.

2. Data analysis

2.1. Out-of-pile test data

The U–Al binary system has three intermetallic compounds, i.e., UAl_2, UAl_3, and UAl_4 [9,10]. UAl_2 has a cubic Laves structure with a lattice parameter of 0.7766 nm. UAl_3 has a $L1_2$ ordered simple cubic structure with a lattice parameter of 0.426 nm. UAl_4 has a body-centered orthorhombic structure with lattice parameters of a = 0.4397 nm, b = 0.6251 nm, and c = 1.3714 nm. The presence of Mo in U introduces a complexity to the interdiffusion behavior of U–Mo vs. Al by forming ternary phases such as $U_6Mo_4Al_{43}$ and UMo_2Al_{20}. $U_6Mo_4Al_{43}$ has a hexagonal structure with lattice parameters of 1.0966 and 1.7690 nm [11]. UMo_2Al_{20} has a cubic structure with a lattice parameter of 1.4506 nm [12].

Several studies are available that characterized the structure of the interaction products formed during out-of-pile diffusion couple tests of U–Mo vs. Al, by using X-ray diffraction (XRD) [13–15]. Fig. 2(a) shows the XRD patterns of the interaction layers of a U–10 wt%Mo atomized fuel dispersed in an Al matrix annealed at 550 °C for 40 h [13]. The diffraction peaks of the UAl_3 and UAl_4

* Corresponding author. Tel.: +82 42 868 8845; fax: +82 42 868 8824.
E-mail address: hjryu@kaeri.re.kr (H.J. Ryu).

0022-3115/$ - see front matter © 2009 Elsevier B.V. All rights reserved.
doi:10.1016/j.jnucmat.2009.01.306

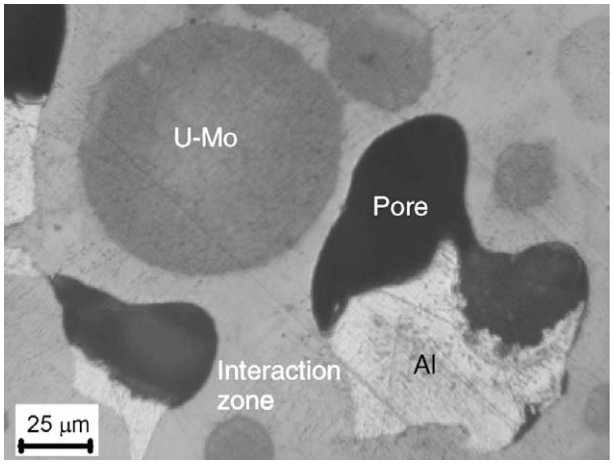

Fig. 1. Microstructure of the U–Mo/Al dispersion fuel: an optical micrograph of an as-irradiated sample.

phases were observed. Mirandou et al. also reported on the observation of UAl_3 and UAl_4 diffraction peaks for the interaction layers of a U–7 wt%Mo vs. Al diffusion couple annealed at 580 °C [14]. They also observed minor peaks of the UMo_2Al_{20} phases in a γ phase U–Mo vs. Al diffusion couple and $U_6Mo_4Al_{43}$ in a decomposed (α + γ′) U–Mo vs. Al diffusion couple. Palancher et al. also detected Al-rich ternary phases, i.e., $U_6Mo_4Al_{43}$ and UMo_2Al_{20}, in U–7 wt%Mo vs. Al diffusion couples annealed at 600 °C for 10 h by using Micro-XRD [15]. They demonstrated that UAl_3 and $U_6Mo_4Al_{43}$, and UAl_4 and UMo_2Al_{20} were strongly correlated by using a micro-XRD mapping. They also proved the very low Mo solubility in the binary phases of UAl_3 and UAl_4 by using a micro-X-ray absorption spectroscopy (XAS).

From out-of-pile annealing tests of U–Mo/Al in a dispersion form [13,16] and diffusion couples of U–Mo vs. Al [13,14], and from casting tests [17], no complete overview of the U–Mo–Al system has yet been established. Recently, Mazaudier et al. deduced phase equilibrium relations for the Mo-deficient part of the U–Mo–Al ternary phase diagram. They determined the diffusion path and explained the observation of periodic layer formation in the diffusion couple based on their phase diagram [18].

As can be seen in the scanning electron microscopy (SEM) image of U–Mo/Al from an annealing test shown in Fig. 2(b), the interaction product on the atomized U–Mo particle consists of multi-layers. Compositions of the interaction products resulting from U–Mo vs. Al diffusion couple tests were obtained from the literature and are marked in the ternary diagram in Fig. 3. In the diffusion couple tests of U–10 wt%Mo vs. Al at 550 °C for 5 h and 25 h, Ryu et al. observed a three-layered interaction zone [13]. The mole ratios of Al to (U + Mo) for 'L1', 'L2' and 'L3' (from the U–Mo side to the Al side) were 3.5, 4.4, and 7.6, respectively. It is considered that the Al-rich layer 'L3', which does not exist in the U–Al binary system, was formed due to the presence of Mo, because the Al/(U + Mo) ratio is similar to the Mo containing ternary compound UMo_2Al_{20}. Mirandou et al. performed diffusion couple tests of U–7 wt%Mo vs. Al at 580 °C for 4 h and found two layers with Al/(U + Mo) ratios of 3.3 and 4.6 [14]. Mazaudier et al. also executed diffusion couple tests of U–Mo with various Mo contents ranging between 5 and 10wt% vs. Al at 600 °C, and noted that the thickness of the Al-rich interaction phase increased with the Mo content [18]. Table 1 lists the compositions of the interaction phases observed by Keiser et al. for diffusion couple tests of U–7Mo vs. Al annealed at 575–650 °C [19]. The Al/(U + Mo) ratios greater than 4 were observed at a higher temperature.

2.2. In-pile test data

Post-irradiation examination (PIE) results of U–Mo/Al dispersion fuel from RERTR tests (in ATR), IRIS-1 and -2 (in OSIRIS), FUTURE (in BR2), and KOMO-1 and -2 (in HANARO), KM003 and KM004 (in VVR), and AECL (in NRU) irradiation tests are available in terms of the compositions of the interaction products [4,6,7,20–22]. Except for the KOMO and AECL tests, which contained a rod-type U–Mo/Al dispersion fuel in a tubular cladding, all the tests were on plate-type fuel. The fuel temperatures for the plate-type fuel tests were below 220 °C; however, those of the central region for some high power rods in the KOMO and AECL tests are well above 220 °C.

The compositions of the interaction layers (Fig. 4 [20]) of the irradiated fuel from the RERTR irradiation tests were measured by Meyer et al. using a wavelength dispersive X-ray spectroscopy (WDS). The Al/(U + Mo) ratio calculated from the measured composition was about 7. Similarly, the composition range of the interaction products for the IRIS-1 test was $(U,Mo)Al_6$–$(U,Mo)Al_7$. The compositions of the interaction zones found in the IRIS-2 test varied depending on their location in a sample with a range of $(U,Mo)Al_{4.4}$–$(U,Mo)Al_{5.8}$ and that from the FUTURE test was

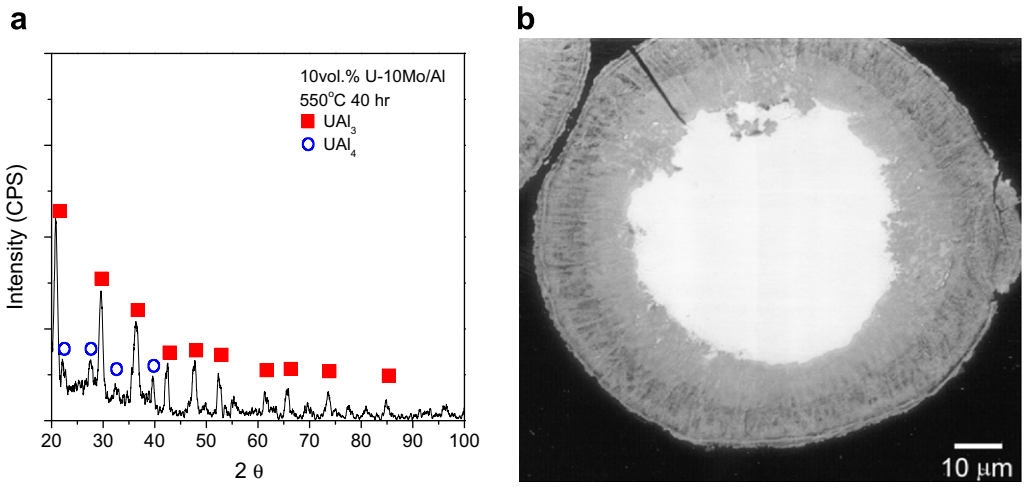

Fig. 2. (a) Scanning electron micrograph of the interaction layers in the U–10Mo/Al dispersion fuel annealed at 550 °C for 25 h, (b) XRD patterns of the interaction layers in the U–10Mo/Al dispersion fuel annealed at 550 °C for 40 h [13].

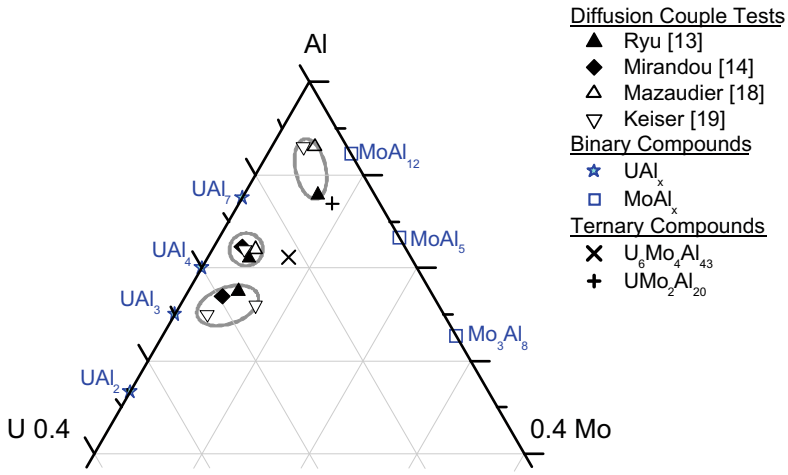

Fig. 3. Part of the U–Mo–Al ternary diagram showing three interaction phase groups based on observations from the out-of-pile U–Mo vs. Al diffusion couple tests. The test temperature ranges from 550–625 °C, which means this ternary diagram is a composite of several isothermal sections.

Table 1
Observed phases in the U–7Mo/Al diffusion couples tests by Keiser et al. [19].

Temperature (°C)	Time (h)	Composition of observed phases (at.%)			
		Al/UMo~2	Al/UMo~3	Al/UMo~4	Al/UMo~7
575	50	$U_{27}Mo_1Al_{72}$	$U_{22}Mo_3Al_{75}$		
575	50	$U_{28}Mo_1Al_{71}$	$U_{17}Mo_7Al_{76}$ $U_{22}Mo_3Al_{75}$		
625	50		$U_{22}Mo_3Al_{75}$	$U_{14}Mo_3Al_{83}$	$U_4Mo_3Al_{93}$

$(U,Mo)Al_{3.3}$–$(U,Mo)Al_{4.7}$ [21]. Table 2 lists the irradiation condition and the composition of the interaction products of the IRIS-1, IRIS-2 and FUTURE tests. The KOMO-2 PIE results show that the interaction layers at the cooler periphery of the fuel rods have higher Al/(U + Mo) ratios, in a range of 3–4.4, than those in the hotter central region of the fuel rods as shown in Fig. 4 [22]. The Al/(U + Mo) ratios of the interaction products formed during irradiation are not as discrete as observed in the out-of-pile diffusion tests, and the microstructure is close to that of a single phase.

Abundant data are available for the reaction of UAl_x (which is a mixture of two or three uranium aluminides, i.e., UAl_2, UAl_3, and UAl_4) and Al in a UAl_x/Al dispersion fuel during irradiation [23–25]. UAl_x/Al dispersion fuel is fabricated by a casting of U–Al or U–Al–Si. The addition of Si into a U–Al alloy stabilizes the UAl_3 phase, preventing a transformation to UAl_4. According to Dienst et al. [23] and Hofman [24], an interaction product forms in a UAl_x/Al dispersion fuel by the reaction of UAl_2 and UAl_3 with Al as shown in Fig. 5. Although, they did not identify the interaction product by a diffraction study, they assumed the interaction phase to be UAl_4 because UAl_4 is the only possible phase higher in Al/U ratio than UAl_2 and UAl_3 according to the U–Al phase diagram. Richt et al. [25] reported on the XRD results of an irradiated 48 wt%U–49 wt%Al–3 wt%Si alloy fuel which is a $U(Al,Si)_3$/Al dispersion. An interaction layer was formed on the $U(Al,Si)_3$ particles. This means that the interaction product must be UAl_4. However, they only observed the UAl_3 phase and the UAl_4 phase was not detected by XRD. The absence of the diffraction pattern of UAl_4 from these tests is indirect evidence that the interaction product is not a crystalline structure. From this review, we found that a high Al-content interaction product, i.e., higher in its Al-content than UAl_3, consistently undergoes amorphization.

More studies on the structure of the interaction products of an irradiated U–Mo/Al dispersion fuel by using the XRD method are to be found in the literature. Dubois et al. reported that they only observed U–Mo and Al diffraction peaks but none for UAl_2, UAl_3 and UAl_4 phases from the samples of the IRIS-1 and IRIS-2 tests [26]. The measured volume fractions of the interaction zones of the IRIS-1 and IRIS-2 tests were 37% and 45%, respectively. Given that the interaction products occupied sufficient volumes to yield a

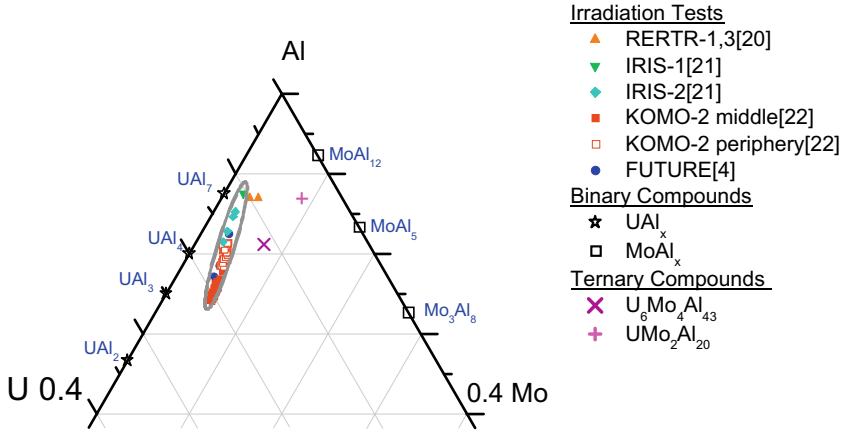

Fig. 4. Part of the U–Mo–Al ternary diagram showing the non-discrete composition variation of interaction products based on observations from the U–Mo/Al irradiation tests at low irradiation temperature.

Table 2
Irradiation conditions and Al/(U + Mo) ratios in the interaction products of the IRIS-1 and -2 [21], FUTURE [4], and KM004 irradiation tests [7].

Test name	Irradiation facility	Heat flux (W/cm^2)	Max. Cladding temperature (°C)	Al/(U + Mo) mole ratio
IRIS-1	OSIRIS	140	75	6–7
KM004	VVR	115	95	4.1–5.7
IRIS-2	OSIRIS	240	100	4.4–5.8
FUTURE	BR2	340	130	3.3–4.7

diffraction peak, the absence of a diffraction peak from the interaction products is another indication that the interaction products are amorphous. Transmission electron microscopy study of the interaction products in an irradiated U–Mo/Al dispersion fuel confirmed that the interaction products that had grown under low temperature irradiation were indeed amorphous [8].

Meanwhile, Conlon and Sears reported on the PIE results of a rod-type U–Mo/Al dispersion fuel irradiated to a 20% ^{235}U burnup [27]. They reported that the diffraction peaks for UAl_2, UAl_3 and UAl_4 were observed from a neutron diffraction analysis (NDA). It is noticeable that the amount of UAl_3 is predominant in the reaction product. They calculated the weight fractions of UAl_2 and UAl_4, by the Rietveld method, to be 1 and 4 wt%, respectively. As Ryu et al. [28] reported the fuel temperature of rod-type fuel with a similar power is much higher, with fuel centerline temperature above 200 °C, than a plate-type fuel, where the fuel temperature ranges from 100–200 °C. Indeed, the post-irradiation micrographs of Colon and Sears exhibited a complete consumption of the U–Mo particles and the Al matrix at the center of the fuel rod. When comparing the burnup and the extent of the interaction between U–Mo and Al with those of KOMO-2, the fuel centerline temperature can be estimated to be close to that of KOMO-2. Therefore, the observation of UAl_4 can be explained by the possibility that the high fuel temperature caused the UAl_4 phase to remain crystalline.

Amorphous UAl_x interaction products can also be found in irradiation tests of U_3Si_2/Al dispersion fuel. In Ref. [29], the U_3Si_2/Al dispersion fuel was irradiated to a 85% U-235 burnup (fission density of $\sim 4.2 \times 10^{21}/cm^3$ fuel) in the ORR (Oak Ridge) and post-irradiation annealed at 400 °C for 700 h. Fig. 6(a) shows an optical micrograph of a U_3Si_2/Al dispersion fuel sample irradiated and then post-irradiation annealed at 400 °C for 700 h. Interaction products of about 4 μm in thickness were observed on U_3Si_2 particles. Because of the relatively low annealing temperature, there was no additional interaction layer growth during the annealing. U_3Si_2 was amorphized during irradiation as shown in 'a' of Fig. 6(b) [30]. Low or high burnup as-irradiated samples do not show any diffraction peaks ('b' and 'c' of Fig. 6(b)). However, after annealing the diffraction peaks of the interaction products (UAl_2 and UAl_3) are detected (d of Fig. 6(b)). Therefore, the diffraction peaks observed after the annealing are due to the restoration of the crystalline structure in the interaction layers by the annealing. The meaning of the test is two folds. One is that the interaction product in U_3Si_2/Al dispersion fuel is amorphous during irradiation. The other is that an annealing at 400 °C can restore the crystalline structure from the amorphous interaction product in U_3Si_2/Al dispersion fuel. The interaction product forming in U_3Si_2/Al dispersion fuel is typically described as $U(Al,Si)_x$. A recent PIE of a test at BR2 showed that the ratio was ~4.6 [31], which is an indication that the interaction layer does not consist of equilibrium phases. Since no U_3Si_2 peaks are observed, even after an annealing at 400 °C, the critical temperature for a crystallization of amorphous U_3Si_2 might be higher than those of UAl_x.

Recent neutron diffraction study revealed that the interaction products of U–Mo/Al dispersion fuel are amorphous [7]. They found that the amorphous interaction products recover their crystalline properties by a high temperature annealing above 350 °C. This means that the amorphous interaction products in this fuel-matrix combination can also be crystallized at a temperature higher than a critical temperature.

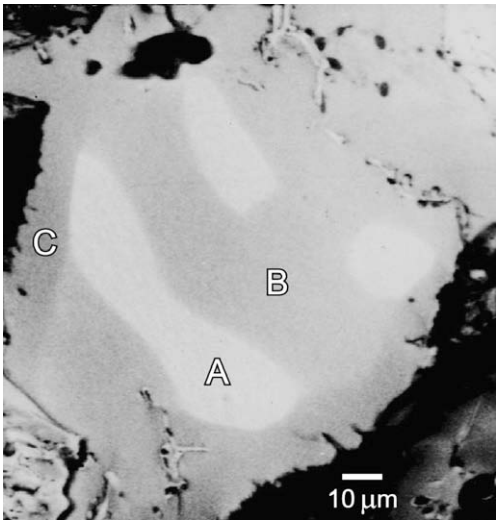

Fig. 5. A scanning electron micrograph of a 93% enriched UAl_x/Al dispersion fuel after a 60% U-235 burnup [24]. A is the UAl_2, B is the UAl_3, C is the interaction product.

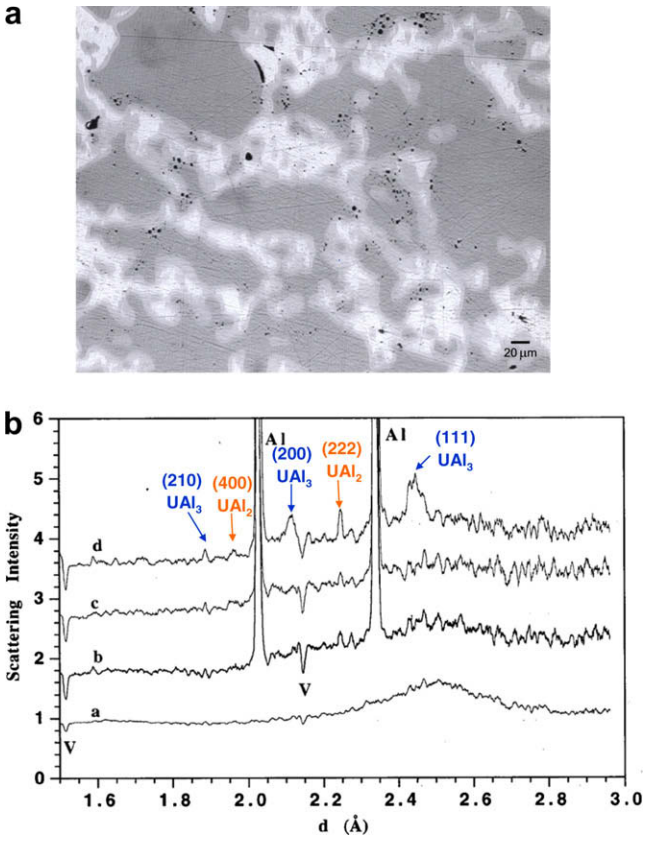

Fig. 6. (a) Optical micrograph of the 5.2 gU/cm^3 LEU U_3Si_2/Al dispersion fuel irradiated to a 85% U-235 burnup in the ORR and post-irradiation annealed at 400 °C for 700 h [29]. (b) Neutron diffraction patterns of the U_3Si_2/Al dispersion fuel. (a: neutron-irradiated U_3Si_2 powder, b: low burnup (45% U-235 burnup) as-irradiated U_3Si_2/Al dispersion fuel, c: high burnup (85% U-235 burnup) as-irradiated U_3Si_2/Al dispersion fuel, d: post-irradiation annealed at 400 °C for 700 h).

The inconsistency regarding the observation of UAl_3 among the test results is attributed to the difference in the irradiation temperature. Irradiation temperature is an important factor in determining whether an interaction product becomes amorphous or remains a crystalline structure. The critical temperature under which an amorphization is possible has been well established from numerous ion irradiation experiments of intermetallic compounds [32].

3. Discussion

The out-of-pile diffusion test results can be summarized as follows: (i) U–Mo vs. Al diffusion couples tend to form multi-layers and each layer consists of multiple phases. (ii) Constituent phases in the reaction zone are UAl_3, UAl_4, $U_6Mo_4Al_{43}$, and UMo_2Al_{20}. (iii) The Al-rich ternary compounds, i.e., an Al/(U + Mo) ratio greater than 4, are the result of multiphase mixtures UAl_4 and UMo_2Al_{20}.

It is remarkable that UAl_2 has not been observed from the diffraction tests of the out-of-pile diffusion couple tests of U–Mo vs. Al. Although, X-ray diffraction peak cannot detect a constituent phase with a small fraction less than about 1 wt%, it is considered that UAl_2 is difficult to form in the diffusion couple tests. The reason may be that the formation kinetics of the UAl_3 phase in the U–Mo vs. Al diffusion couple tests is more favorable than the UAl_2 phase. UAl_2 phase only formed when the Al matrix was completely consumed as observed from an annealing test of U_3Si/Al and U_3Si_2/Al dispersion fuels at 600 °C for 33 days with a 50-vol% fuel loading [33]. In these fuels UAl_3 is normally the phase that forms as long as the Al matrix remains.

A comparison of the interdiffusion behavior is given in Figs. 3 and 4 and reveals a remarkable difference between the out-of-pile and in-pile tests. In Fig. 3, composition data are spread among several equilibrium phases whereas those in Fig. 4 lie along a narrow band. The fundamental reason is that the interaction products from the out-of-pile tests were crystalline and thermodynamically stable phases, whereas those of the low irradiation temperature in-pile tests were non-equilibrium mixtures of U, Mo and Al due to irradiation damage. In this situation, the interaction products remain as non-equilibrium mixtures of U, Mo and Al where the Al/(U + Mo) ratio of the interaction products does not need to be an integer as in out-of-pile case.

Table 2 compares irradiation conditions of the various tests (IRIS-1, KM004, IRIS-2, and FUTURE) and the compositions of resultant interaction products. The characteristics of the amorphous interaction products formation in U–Mo/Al could be summarized as follows: (i) As the fuel temperature increases, the average Al/(U + Mo) atom ratio of the interaction products decreases. (ii) As the test temperature decreases, amorphous interaction products tend to form. In other words, crystalline interaction products tend to form under high temperature irradiation. (iii) Although a subtle difference, an interaction product with a Al/(U + Mo) ratio greater than 3 seems to be amorphized with more ease, based on the fact that the interaction products on UAl_3 are amorphous and that UAl_3 is crystalline at the same irradiation dose.

In addition to the absence of diffraction peaks, the variation of the composition is a feature of an amorphous interaction product of U–Mo/Al dispersion fuel. The composition of an interaction product has a relation with the fuel temperature. The fuel temperature for the IRIS-1 test is the lowest, that for the IRIS-2 and KM004 is higher, and that for the FUTURE is the highest. This means that, the hotter the fuel is, the lower the Al/(U + Mo) ratio is for the irradiation tests. The representative ratio for the out-of-pile tests ranges from 3 to 4.4 in accordance with the phase diagram of the U–Al system, whereas ratios from 3.3 to 7 are observed in the in-pile tests. This difference can be explained by the fact that the interaction products are in a non-equilibrium state during irradiation.

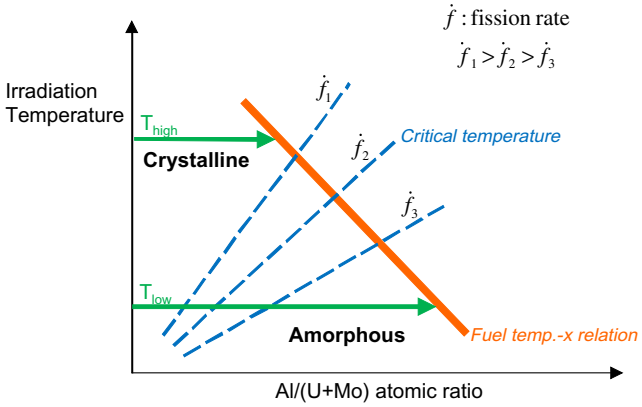

Fig. 7. Schematic diagram illustrating the concept of the critical temperature for an amorphization of an interaction product during irradiation.

Fission fragment damage has a greater effect on the process of amorphization of the interaction products than thermodynamic constraints, particularly at low temperatures. When an interaction product becomes amorphous, U, Mo and Al exist as a non-equilibrium mixture. In this situation, because of the fission-fragment damage causing a structural strain related to defects and disorder, the Al/(U + Mo) ratio can be higher than that possible for the out-of-pile tests. On the other hand, when the fuel temperature increases sufficiently for the interaction product to devitrified to a crystalline structure, the ratio decreases to 3 similar to the out-of-pile cases because the $(U,Mo)Al_3$ type interaction product is thermodynamically more favorable. For this reason, the rod-type U–Mo/Al dispersion fuel irradiated at a high temperature above 400 °C reveal crystalline UAl_3 diffraction peaks. A satisfactory explanation for the seemingly contradicting observations from the out-of-pile tests and the in-pile tests is only possible when the interaction products formed at low temperature are in fact in the amorphous state [34].

The factors determining whether an interaction product is crystalline or amorphous are irradiation temperature, the damage rate in an interaction product, which is proportional to the fission rate in adjacent fuel particles. Competition between the thermal annealing rate and the damage rate controls the amorphization during irradiation [32]. At high temperatures, thermal annealing facilitates recovery of damage. In contrast, a high fission rate produces more defects and disorder. The relation between the temperature and fission rate coupled with the Al/(U + Mo) ratio is schematically illustrated in Fig. 7. The critical temperature depends on

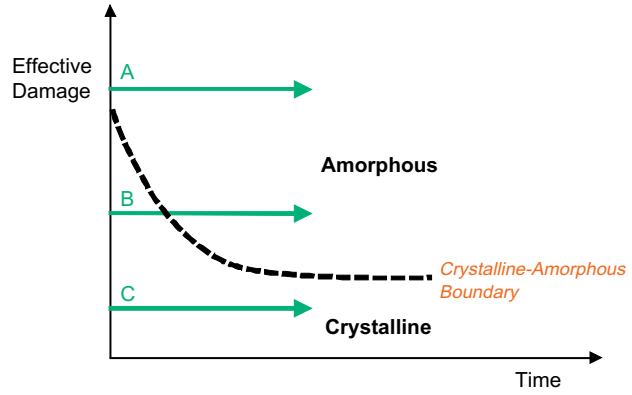

Fig. 8. Schematic diagram illustrating three possible cases of interaction product formation according to an effective damage factor during irradiation. Case A is amorphous interaction product formation, Case B is crystalline to amorphous transformation of interaction product, and Case C is crystalline interaction product formation.

the fission rate and the Al/(U + Mo) ratio is a function of the fuel temperature. Considering that UAl_x is more difficult to amorphize than U_3Si_2 [29] and the critical temperature for an amorphization of U_3Si_2 is 250 °C [30], the critical temperature for the amorphization of an interaction product in a U–Mo/Al dispersion fuel is estimated to be less than 250 °C.

The question as to whether the interaction product is crystalline or amorphous at the time of its initial formation remains open at the moment because no experimental evidence is available. Because the tests in the literature focused on an amorphization of initially crystalline samples during irradiation, this question has never been answered. However, the present study deals with the situation in which the object material is newly formed during irradiation. As schematically illustrated in Fig. 8, there are three possible regimes of an irradiation condition in terms of the effective damage factor which is a function of the damage rate and the irradiation temperature. When the irradiation condition is overwhelmingly favorable for the formation of an amorphous interaction product and in particular the observed composition is thermodynamically infeasible, the interaction product is amorphous from the initial stage (Regime A in Fig. 8). However, when the irradiation condition is not so favorable as in the above case for the amorphous interaction product formation, it is possible that the initial interaction product is crystalline and then becomes amorphous after accumulating enough radiation damage (Regime B in Fig. 8). When the irradiation condition is weak (Regime C in Fig. 8), the interaction product remains crystalline after the irradiation test.

4. Conclusions

The differences in the interdiffusion behavior of U–Mo vs. Al between the out-of-pile and in-pile tests are mainly due to the differences in the structures of the interaction products. The interaction products from the out-of-pile tests are determined thermodynamically and are crystalline. The differences between the in-pile test results and the out-of-pile results can only be explained when the interaction products from the in-pile tests are non-equilibrium mixtures resulted from irradiation damage.

The composition (or Al/(U + Mo) ratio), the irradiation temperature, and the fission rate are the three most important factors for determining whether an interaction product is amorphous or crystalline. The higher the Al/(U + Mo) ratio, the lower the temperature, and the higher the fission rate, the easier the amorphous interaction product formation is. The critical temperature for the amorphous interaction product formation is also dependent on the fission rate and the composition of an interaction product.

Acknowledgments

One of the authors is grateful for the support of the National Nuclear Research Program by the Ministry of Education, Science and Technology of Korea (MEST) and the Korea Research Foundation Grant with the Grant number of KRF-2005-214-D00116.

References

[1] J.L. Snelgrove, G.L. Hofman, M.K. Meyer, C.L. Trybus, T.C. Wiencek, Nucl. Eng. Design 178 (1997) 119.
[2] M.K. Meyer, G.L. Hofman, S.L. Hayes, C.R. Clark, T.C. Wiencek, J.L. Snelgrove, R.V. Strain, K.H. Kim, J. Nucl. Mater. 304 (2002) 221.
[3] G.L. Hofman, Y.S. Kim, M.R. Finlay, J.L. Snelgrove, C. Clark, in: Proceedings 2003 International RERTR Meeting, Chicago, IL, USA, 2003. Available from: <http://www.rertr.anl.gov/index.html>.
[4] A. Leenaers, S. Van den Berghe, E. Koonen, C. Jarousse, F. Huet, M. Trotabas, M. Boyard, S. Guillot, L. Sannen, M. Verwerft, J. Nucl. Mater. 335 (2004) 39.
[5] G.L. Hofman, Y.S. Kim, Nucl. Eng. Technol. 37 (2005) 299.
[6] K. Colon, D. Sears, in: Transactions of RRFM-2007, Lyon, France, 11–15th March, 2007. Available from: <http://www.rrfm2007.org>.
[7] O.A. Golosov, V.B. Semerikov, A.E. Teplykh, M.S. Lyutikova, E.F. Kartashev, V.A. Lukichev, in: Transactions of RRFM-2007, Lyon, France, 11–15th March, 2007. Available from: <http://www.rrfm2007.org>.
[8] S. Van den Berghe, W. Van Renterghem, A. Leenaers, J. Nucl. Mater. 375 (2008) 340.
[9] R.E. Rundle, A.S. Wilson, Acta Crystallogr. 2 (1949) 148.
[10] M.E. Kassner, P.H. Adler, M.G. Adamson, D.E. Peterson, J. Nucl. Mater. 167 (1989) 160.
[11] S. Niemann, W. Jeitschko, Z. Metallkd. 85 (1994) 345.
[12] S. Niemann, W. Jeitschko, J. Solid State Chem. 114 (1995) 337.
[13] H.J. Ryu, Y.S. Han, J.M. Park, C.K. Kim, S.D. Park, J. Nucl. Mater. 321 (2003) 210.
[14] M.I. Mirandou, S.N. Balart, M. Ortiz, M.S. Granovsky, J. Nucl. Mater. 323 (2003) 29.
[15] H. Palancher, P. Martin, V. Nassif, R. Tucoulou, O. Proux, J.-L. Hazemann, O. Tougait, E. Lahéra, F. Mazaudier, C. Valot, S. Dubois, J. Appl. Cryst. 40 (2007) 1064.
[16] H.J. Ryu, Y.S. Kim, G.L. Hofman, J.M. Park, C.K. Kim, J. Nucl. Mater. 358 (2006) 52.
[17] D.D. Keiser, C.C. Clark, M.K. Meyer, Scripta Mater. 51 (2004) 893.
[18] F. Mazaudier, C. Proye, F. Hodaj, J. Nucl. Mater. 377 (2008) 476.
[19] D.D. Keiser, Argonne National Laboratory Report, ANL-05/14, July, 2005.
[20] M.K. Meyer, G.L. Hofman, R.V. Strain, C.R. Clark, J.R. Stuart, in: Proceedings 2000 International RERTR Meeting, Las Vegas, Nevada, USA, 1–6th October, 2000. Available from: <http://www.rertr.anl.gov/index.html>.
[21] F. Huet, J. Noirot, V. Marelle, S. Dubois, P. Boulcourt, P. Sacristan, S. Naury, P. Lemoine, in: Transactions of RRFM-2005, Budapest, Hungary, 10–13th April, 2005. Available from: <http://www.rrfm2005.org>.
[22] J.M. Park, H.J. Ryu, Y.S. Lee, D.B. Lee, S.J. Oh, B.O. Yoo, Y.H. Jung, D.S. Sohn, C.K. Kim, in: Proceedings 2004 International RERTR Meeting, Vienna, Austria, 7–12th November, 2004. Available from: <http://www.rertr.anl.gov/index.html>.
[23] W. Dienst, S. Nazare, F. Thummler, J. Nucl. Mater. 64 (1977) 1.
[24] G.L. Hofman, Nucl. Technol. 77 (1987) 110.
[25] A.E. Richt, C.F. Leitten, R.J. Beaver, Research Reactor Fuel Element Conference, Gatlinburg, TN, 17–19th September, 1962.
[26] S. Dubios, J. Noirot, J.M. Gatt, M. Ripert, P. Lemoine, P. Boulcourt, in: Transactions of RRFM-2007, Lyon, France, 11–15th March, 2007.
[27] K.T. Conlon, D. Sears, in: Transactions of RRFM-2006, Sofia, Bulgaria, April 30–May 3, 2006. Available from: <http://www.rrfm2006.org>.
[28] H.J. Ryu, J.M. Park, C.K. Kim, H.T. Chae, Y.S. Kim, Nucl. Eng. Technol. 40 (2008) 409.
[29] G.L. Hofman, Argonne National Laboratory, 1987, unpublished data.
[30] R.C. Birtcher, J.W. Richardson, M.H. Mueller, J. Nucl. Mater. 230 (1996) 158.
[31] A. Leenaers, E. Koonen, Y. Parthoens, P. Lemoine, S. Van den Berghe, J. Nucl. Mater. 375 (2008) 243.
[32] A.T. Motta, J. Nucl. Mater. 244 (1997) 277.
[33] S. Nazare, J. Nucl. Mater. 124 (1984) 14.
[34] H.J. Ryu, Y.S. Kim, G.L. Hofman, D.D. Keiser, in: Proceedings 2006 International RERTR Meeting, Cape Town, South Africa, October 29–November 2, 2006. Available from: <http://www.rertr.anl.gov/index.html>.